EFDA–JET–CP(11)04/26

J. Citrin, J. Hobirk, M. Schneider, J.F. Artaud, C. Bourdelle, K. Crombe,
G.M.D. Hogeweij, F. Imbeaux, E. Joffrin, F. Koechl, J. Stober,
the AUG team and JET EFDA contributors

Predictive Transport Analysis of JET and AUG Hybrid Scenarios

Predictive Transport Analysis of JET and AUG Hybrid Scenarios

J. Citrin[1], J. Hobirk[2], M. Schneider[3], J.F. Artaud[3], C. Bourdelle[3], K. Crombe[4], G.M.D. Hogeweij[1], F. Imbeaux[3], E. Joffrin[5], F. Koechl[6], J. Stober[2], the AUG team and JET EFDA contributors*

JET-EFDA, Culham Science Centre, OX14 3DB, Abingdon, UK

[1]FOM Institute for Plasma Physics Rijnhuizen, Association EURATOM-FOM, Nieuwegein, The Netherlands
[2]MPI für Plasmaphysik, EURATOM Association, Boltzmannstr. 2, 85748 Garching, Germany
[3]CEA, IRFM, F-13108 Saint Paul Lez Durance, France
[4]Department of Applied Physics, Ghent University, Rozier 44, 9000 Ghent, Belgium
[5]JET-EFDA-CSU, Culham Science Centre, Abingdon, OX14 3DB, UK
[6]Association EURATOM-ÖAW/ATI, Atominstitut, TU Wien, 1020 Vienna, Austria
** See annex of F. Romanelli et al, "Overview of JET Results", (23rd IAEA Fusion Energy Conference, Daejon, Republic of Korea (2010)).*

Preprint of Paper to be submitted for publication in Proceedings of the
38th EPS Conference on Plasma Physics
Strasbourg, France
(27th June 2011 - 1st July 2011)

INTRODUCTION

Hybrid scenarios in present machines are characterized by improved confinement compared to the IPB98(y,2) empirical scaling law expectations. A number of possibilities explaining this improvement have been proposed: reduction in deleterious MHD, pedestal confinement improvement, rotational shear turbulence suppression, increased turbulent thresholds due to qprofile shaping, and stiffness reduction at low magnetic shear [1, 2, 3]. This work concentrates on isolating the impact of increased s/q at outer radii (where s is the magnetic shear) on core confinement in low-triangularity JET and ASDEX Upgrade (AUG) experiments. This is carried out by predictive heat and particle transport modelling using the integrated modelling code CRONOS [4] coupled to the GLF23 turbulent transport model [5]. This work aims to validate recent predictions of the ITER hybrid scenario also employing CRONOS/GLF23, where a high level of confinement and resultant fusion power sensitivity to the s/q profile was found [6].

1. EXPERIMENTAL DISCHARGES

For both machines, discharge pairs were analyzed displaying similar pedestal confinement yet significant differences in core confinement. A variation in q-profile was experimentally achieved in each pair, via the 'current-overshoot' method for the JET case (Pulse No's: 79626/79630, with $B_T = 2T$, $I_P = 1.7MA$ and $\beta_N(W_{th}) = 1.9/2.1$, $\beta_N(W_{dia}) = 2.6/2.8$) [7, 1], and by varying the auxiliary heating timing in the AUG case (20993/20995, with $B_T = 2.4T$, $I_P = 1MA$, and $\beta_N(W_{th}) = 1.6/1.9$, $\beta_N(W_{dia}) = 1.9/2.3$) [8]. Temporal evolution of the total plasma current, heating powers and confinement factors ($H_{98} \equiv \tau_{th}/IPB98(y,2)$) can be seen in figure 1. The s/q and rotation profiles used throughout this analysis can be seen in figure 2. For the JET pair, the interpretative q-profiles were used since the transient effect of the current overshoot may in certain cases be within the error bars of the MSE measurements. For the AUG pair, the measured q-profiles were used since the interpretative q-profiles failed to reproduce the measured relaxed q-profiles within experimental error, and MHD activity may be redistributing the current, clamping the q-profile to 1. The rotation profiles for the JET case are similar. For the AUG case, the 20993 (lower confinement) case has a significantly flatter rotation profile in the low magnetic shear region $x<0.4$. Finally, all discharges are devoid of NTMs in the temporal periods studied, apart from AUG 20993, which has a 3/2 NTM in the vicinity of $x = 0.5$.

2. MODELLING TOOLS AND TECHNIQUES

The core of CRONOS is a 1.5D transport solver, whereby 1D current diffusion, particle and energy equations are solved up to the separatrix, self consistentlywith 2Dmagnetic equilibrium. The NBI heat and current sources are calculated by NEMO/SPOT [9]. In all simulations, GLF23 is employed within the region $x = 0–0.83$, where x is the normalized toroidal flux coordinate. For each discharge, comparison simulations were carried out substituting the qprofile input with the q-profile from the other member of each pair. In such a manner GLF23 predicts the confinement difference solely

due to the q-profile. Further linear threshold analysis examining the effect of s/q is also carried out with the quasilinear gyrokinetic transport model QuaLiKiz [10].

3. RESULTS

Figure 3 shows the T_i predictions for JET Pulse No: 79630. These simulations include *heat transport only*, and runs were carried out both with and without E×B suppression. Pulse No: 79630 simulations with the substituted q-profile from Pulse No: 79626 (the improved confinement case) are also shown.

The inclusion of E×B suppression leads to overprediction of T_i. This overprediction is also seen in JETTO [11] simulations of the same discharge, displayed in the same figure. However, independently of the degree of prescribed E×B suppression, the q-profile substitution leads to a degree of T_i increase comparable to the experimentally observed difference. A more quantitative analysis of these differences, and of all subsequent simulations discussed below, can be found in table 1. This pattern is replicated in the AUG simulations, displayed in figure 4 for a heat transport simulation of shot 20995. In the AUG case the degree of Ti overprediction is more severe. However, regardless of the E×B suppression assumption, the q-profile substitution leads to a T_i difference consistent with observations.

In figure 5, the results of *combined heat and particle transport* simulations for JET Pulse No: 79630 are shown. The pattern remains similar to the heat transport only cases, although the primary effect on confinement improvement following the q-profile substitution is now in the particle channel. The reduction of the Ti gradient increase in comparison to the heat transport only case, is due to positive correlation in GLF23 between density gradients and transport, interpreted as the destabilization of TEM modes. Similar results are shown for AUG 20995 in figure 6.

For the AUG case, the degree of improved particle transport is consistent with observation, although when E×B suppression is included the ne profiles are significantly overpredicted. In table 1 the simulation results are summarized in terms of the predicted core thermal energy content: $W_{core} = \int_0^{xped} (P_{th}(x) - P_{th}(x_{ped}))Jdx$, where x_{ped} is taken at the GLF23 operational zone boundary at $x = 0.83$, and J the Jacobian corresponding to the volume element. The table summarizes - according to GLF23 - the extent of the s/q effect *alone* in explaining the core confinement *differences* between each pair, both including and excluding E×B shear stabilization.

Finally, additional analysis was carried out for the JET case with QuaLiKiz, where we assess the sensitivity of the instability linear thresholds to the q-profile, at $x = 0.65$. The experimental R/L_{Ti} is 5.9±0.5 and 6.3±0.3 for Pulse No's: 79630 and 79626 respectively, calculated with respect to a radial coordinate defined as $(R_{in} - R_{out})/2$, where $R_{in,out}$ are the radii to the high field and low field side flux surfaces on the midplane. If we take R_{out} as the radial coordinate, the gradients rise to 7.5±0.6 and 8.1±0.4. QuaLiKiz predicts $R/L_{Ti} = 7.32$ for Pulse No: 79630, and $R/L_{Ti} = 8.08$ for the same input apart from the substitution of the Pulse No: 79626 q-profile and magnetic shear values. The experimental R/L_n(e,i) values were 2.6/2.9, and R/L_{Te} was kept at the observed ratio to R/L_{Ti} throughout the R/L_T scan.

DISCUSSION AND CONCLUSIONS

A significant proportion of improved confinement in the JET and AUG hybrid scenarios analysed here is due to improved q-profile shaping in the high magnetic shear region, at $x > 0.4$, according to GLF23. A proportion of 60/30% of the observed improvement in core thermal energy content within each JET/AUG pair respectively, is predicted through q-profile substitution alone (when averaging the ratios in the bottom line of table 1). In the heat transport simulations, differences in R/L_{Ti} are in the JET case only observed in the high shear region ($x > 0.4$) and are correlated with differences in s/q. In the AUG case, the R/L_{Ti} differences occur both in the low and high magnetic shear regions within $x = 0.3-0.6$. The R/L_{Ti} difference in the high shear region is correlated with a difference in s/q. However, the difference in the low shear region cannot be explained by s/q effects. Due to the difference in rotational shear for $x < 0.4$ between the two discharges in the AUG case, it may be possible that reduced stiffness in the low shear region (not predicted by the stiff GLF23) may account for a further proportion of core confinement difference, as also observed in JET [3]. It is also possible that the 3/2 NTM observed in AUG 20093 is partially responsible for the apparent overprediction of the core confinement by GLF23, even when not including ExB shear suppression, and can thus explain a proportion of the core energy content difference between the pair. Including rotation in GLF23 leads to core energy content overprediction for all discharges, although it is not possible to verify whether this is due to the GLF23 E×B shearing model or to an intrinsic overprediction of the turbulent thresholds. Nevertheless, confinement improvement due to s/q is independent of the rotation assumption. The degree of improvement in the ITG/TEM linear thresholds in the JET pair is also well predicted by QuaLiKiz through the s/q effect. The overlap of the experimental error bars on R/L_{Ti} is however a caveat in such analysis.

REFERENCES

[1]. E. Joffrin et al., in Fusion Energy 2010 (Proc. 23rd Int. Conf. Daejeon, 2010) (Vienna: IAEA).
[2]. C.F. Maggi et al., Nuclear Fusion **50** (2010) 025023.
[3]. P. Mantica et al., this conference.
[4]. J.F. Artaud et al., Nuclear Fusion **50** (2010) 043001.
[5]. J.E. Kinsey et al. Physics of Plasmas **12** (2005) 052503.
[6]. J. Citrin et al., Nuclear Fusion **50** 9 (2010) 115007.
[7]. J. Hobirk et al., submitted to Plasma Physics and Controlled Fusion
[8]. J. Stober et al., Nuclear Fusion **47** 7 (2007) 728.
[9]. M. Schneider et al., Nuclear Fusion **49** 7 (2009) 125005.
[10]. C. Bourdelle et al., Physics of Plasmas **47** 14 (2007) 112501.
[11]. G. Cenacchi et al., ENEA RT/TIB/88/5 (1988).

	EXP	Heat transport		Heat and particle			EXP	Heat transport		Heat and particle	
		no E×B	with E×B	no E×B	with E×B			no E×B	with E×B	no E×B	with E×B
79630 (q30)	1.67	1.71	2.37	1.71	2.68	20995 (q95)	0.33	0.36	0.48	0.34	0.47
79626 (q26)	1.97	1.9	2.62	1.83	3.03	20995 (q93)	0.22	0.3	0.43	0.29	0.41
Ratio	1.17	1.11	1.11	1.07	1.13	Ratio	1.5	1.2	1.12	1.17	1.15

Table 1: Core thermal energy following GLF23 predictions for JET and AUG hybrids. Units are [MJ].

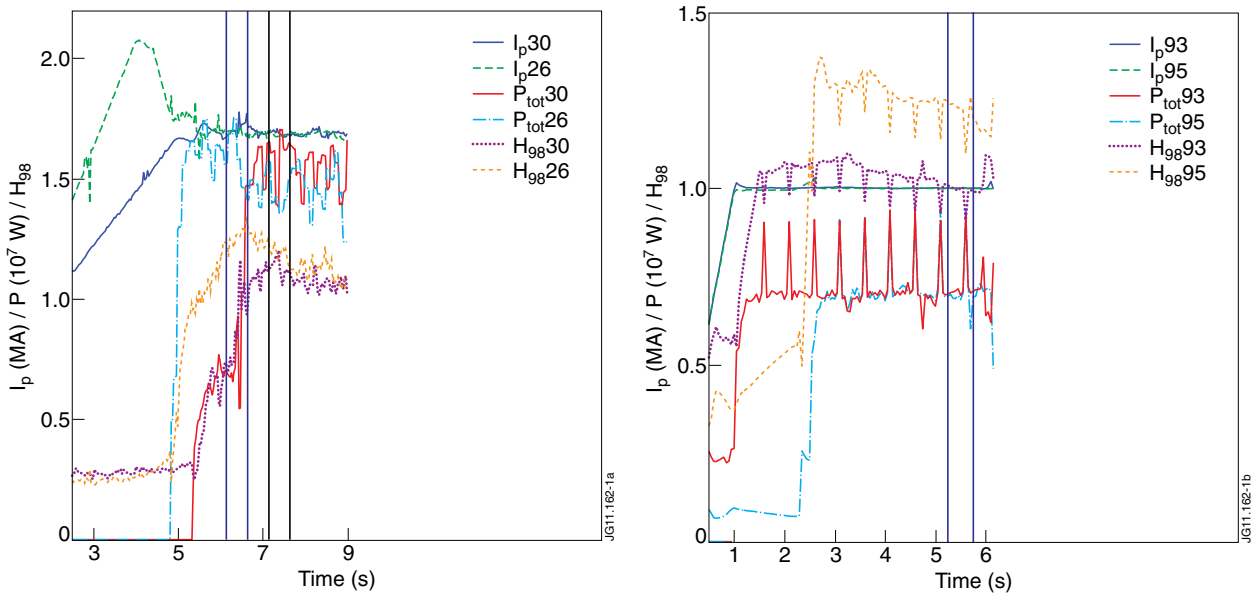

Figure 1: Evolution of I_p[MA], P_{tot} [10^7W] and H_{98} for the JET (left panel) and the AUG (l panel) pairs.

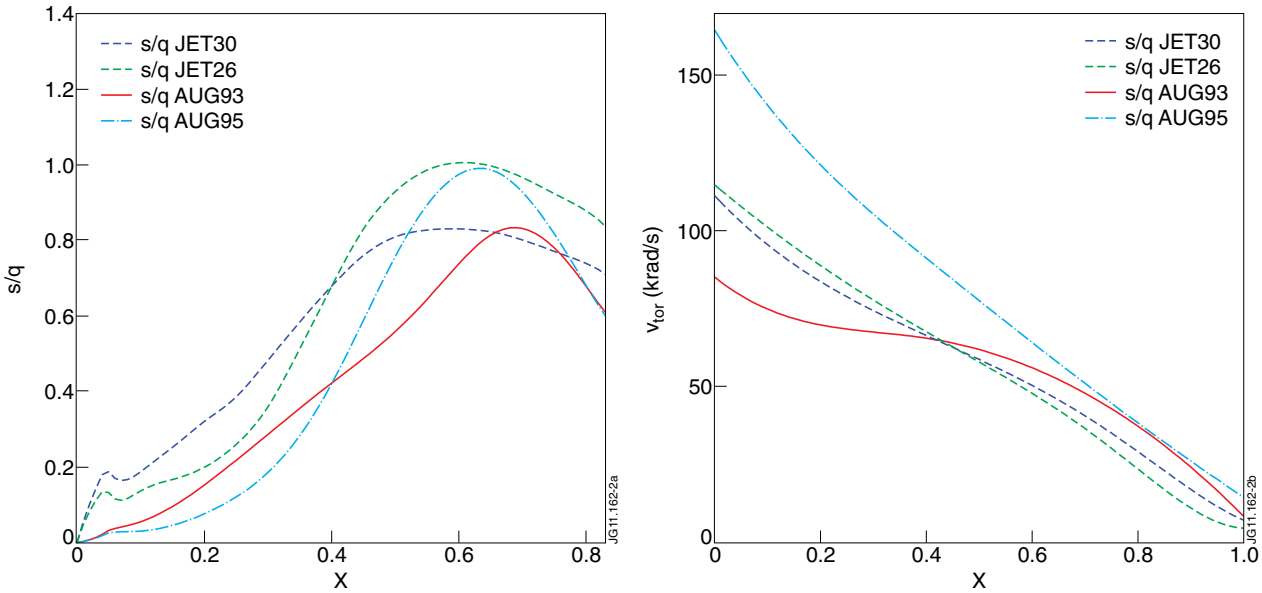

Figure 2: s/q (left) and rotation (right) profiles for all analysed discharges.

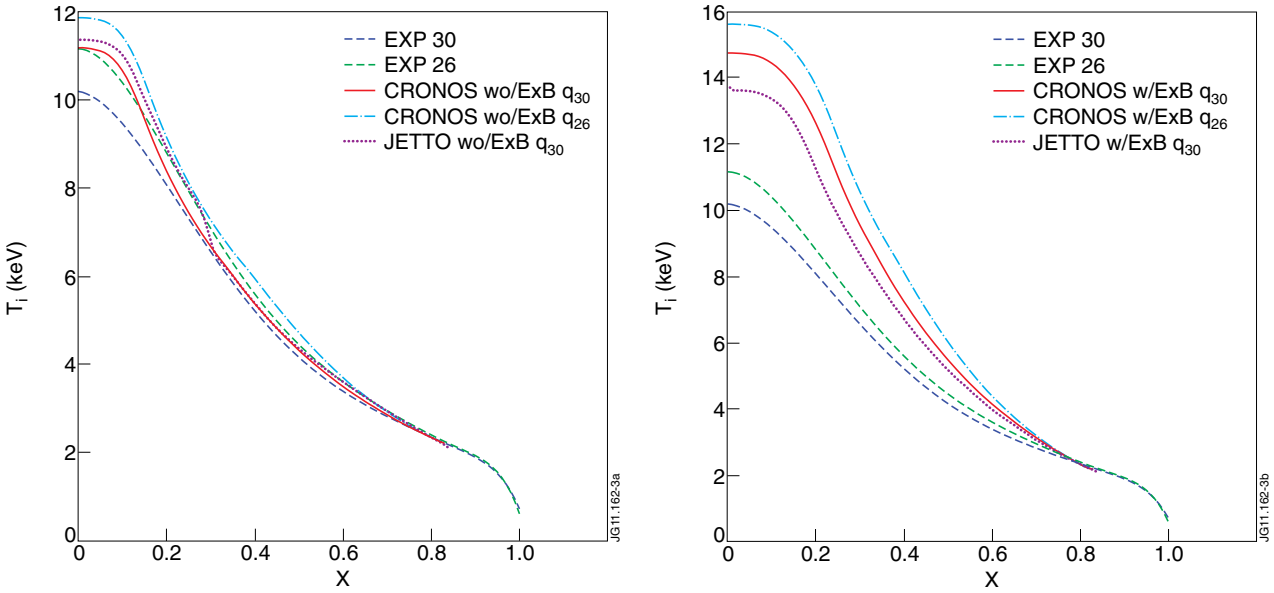

Figure 3: Heat transport only GLF23 predictions for ion temperatures in JET Pulse No: 79630, excluding E×B suppression (left panel) and including E×B suppression (right panel), and with the substituted q-profile from Pulse No: 79626.

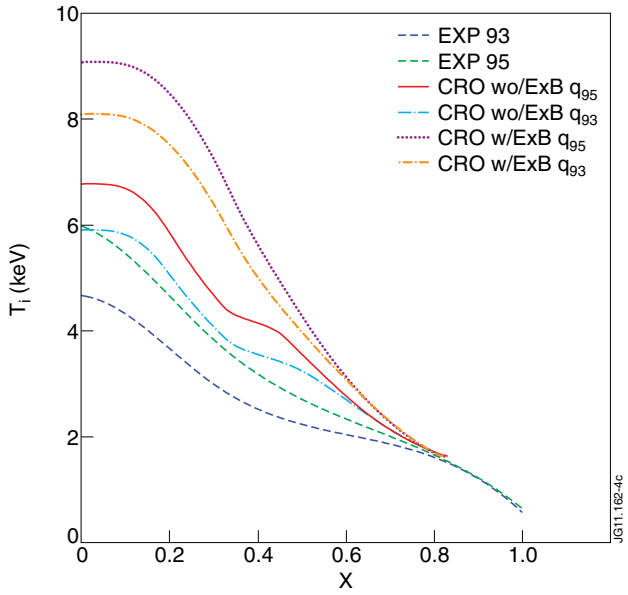

Figure 4: Heat transport only GLF23 predictions for ion temperatures in AUG 20995.

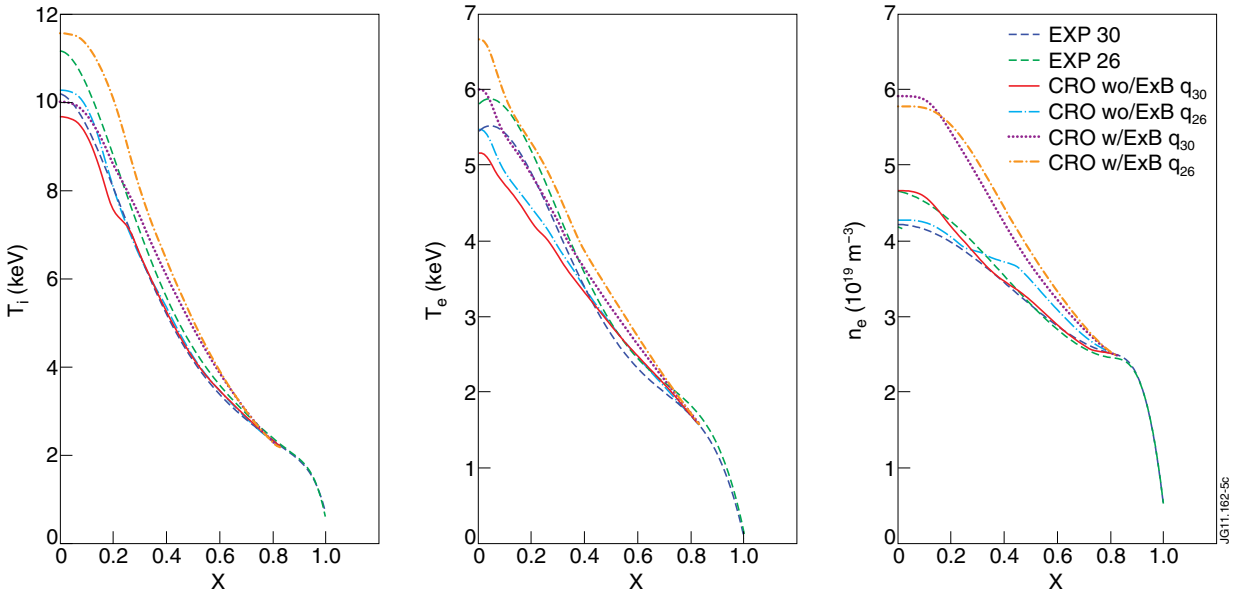

Figure 5: Heat and particle transport GLF23 predictions of T_i (left panel), T_e (center panel), and ne (right panel) for JET Pulse No: 79630.

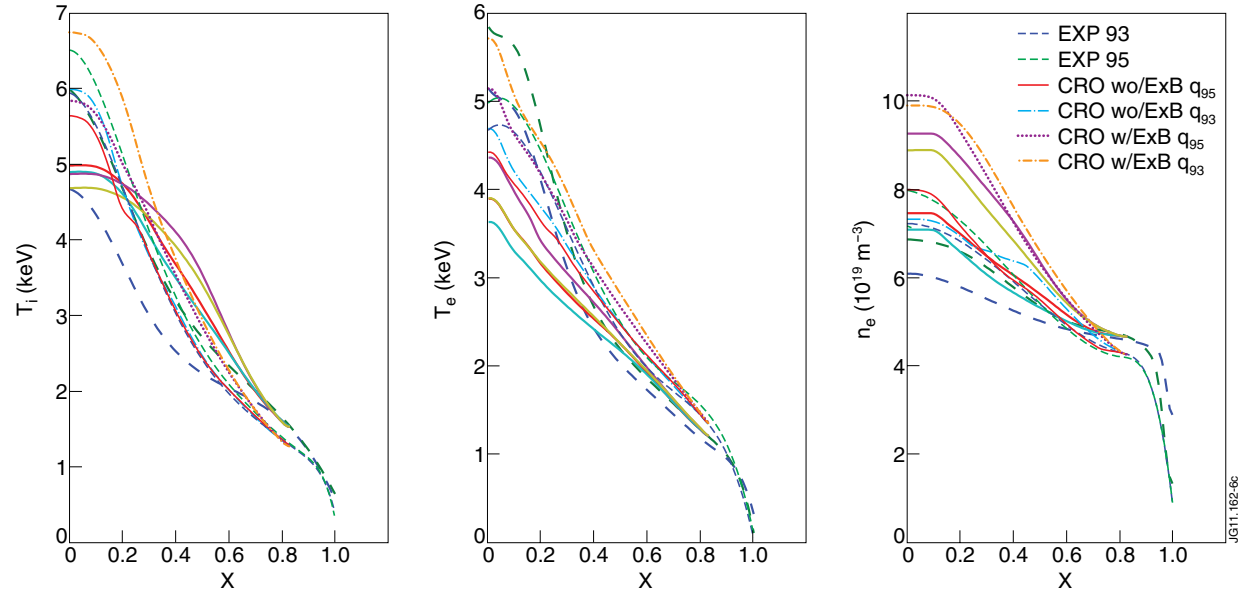

Figure 6: Heat and particle transport GLF23 predictions of T_i (left panel), T_e (center panel), and n_e (right panel) for AUG 20995.